Dynamic modelling of battery energy storage system and application to power system stability

C.-F. Lu
C.-C. Liu
C.-J. Wu

Indexing terms: Battery energy storage, Power system stability

Abstract: A useful and systematic dynamic model of a battery energy storage system (BES) is developed for a large-scale power system stability study. The model takes into account converter equivalent circuits, battery characteristics and internal losses. Both charging mode and discharging mode are presented. The model is expressed in equivalent transfer function blocks, and it can be easily used in dynamic stability analysis of a power system. To examine the dynamic behaviour of the model, applications to the damping of turbogenerator torsional oscillations are performed. Active and reactive power modulation by the BES can be controlled according to system requirements. Eigenvalue analysis and dynamic simulations are performed to demonstrate the damping effect of the BES.

List of principal symbols

E_{DO}	= ideal no-load maximum DC voltage of converter
V_t	= BES terminal voltage
V_{BT}	= average DC voltage of battery
R_{BT}, R_{BS}	= battery connecting resistance and internal resistance
X_{CO}	= converter commutating reactance
I_{BES}, P_{BES}, Q_{BES}	= BES current, active power, and reactive power
P_{DC}, Q_{DC}	= DC active power and reactive power of battery
V_{B1}	= battery overvoltage
R_{B1}, C_{B1}	= resistance and capacitance at charging and discharging procedures
R_{BP}	= battery self-discharge resistance
C_{BP}	= battery capacitance
V_{BOC}	= battery open-circuit voltage
K_{BP}, T_{BP}	= speed measurement device gain and time constant
K_{BQ}, T_{BQ}	= voltage measurement device gain and time constant
K_M	= feedback factor of BES
K_R, T_R	= firing circuit gain and time constant
U_{BES}	= auxiliary controller output signal
K_W, T_W, T_1, T_2	= parameters of auxiliary lead–lag controller
α_R, β_I	= converter firing angle and ignition advance angle
ϕ_R, ϕ_I	= power phase angles of charging and discharging battery
ω	= generator rotor speed

Paper 1858C (P9, P10), first received 18th April 1994 and in revised form 10th January 1995

C.-F. Lu and C.-C. Liu are with the Department of Electrical Engineering, National Taiwan University, Taipei, Taiwan, Republic of China

C.-J. Wu is with the Department of Electrical Engineering, National Taiwan Institute of Technology, 43, Keelung Road Section 4, Taipei 106, Taiwan, Republic of China

1 Introduction

At present, electric power consumption patterns have resulted in increasingly large differences between day and night energy demands owing to the high electrification of customers. In summer the air-conditioning load is about 30% of the Taiwan power system peak load. How to effectively use or store off-peak energy to meet peak energy demand has received substantial attention in electric utilities. In addition to better use of energy resources, improving system performances and possible implementation, a battery energy storage system (BES) has the following features

(*a*) modularity
(*b*) environmentally benign
(*c*) high efficiency
(*d*) quick response

In the past decades, almost all investigations concentrated upon these topics concerning the well-known applications of a BES: peak-shaving [1, 2] or load frequency control [3]; and system planning, such as capacity decision, economic assessment and location. Although load-levelling is the original purpose of a BES, it also can be used as a stabiliser of power systems [4]. The dynamic damping improvement must be an additional benefit from the BES but not the only one, since the BES must be primarily used for load management.

Dynamic modelling of a BES was first proposed by Carroll *et al.* [5, 6]. The equivalent circuit of batteries was represented by a constant voltage source behind a parallel *RC* circuit, i.e. a Thevenin equivalent circuit. Although this model can describe the outer behaviour of a BES correctly during dynamic period, it is incomplete in the inner interaction of a BES, since the voltage of a BES is not constant. The voltage of a BES is dependent on the operating conditions. The studies in this paper combine the characteristics of the converter [6, 7] and the battery equivalent circuits [8, 9] to construct a dynamic model of a BES. The detailed interaction between components is presented. The difference of a BES in charging and discharging modes is compared.

Although high-order models which account for nonlinearities have already been developed and are in commercial applications, a BES dynamic model which can be used in the stability analysis of a large-scale power system is also required.

To examine the dynamic responses of the BES model, applications of this model to improve power system stability are investigated. This paper is thought to be the first attempt at damping torsional oscillations by a BES. The damping effect on low-frequency oscillations is also observed. Both eigenvalues analysis and nonlinear time-domain simulations are performed on the IEEE Second Benchmark Model, system 1 [10]. A simple first-order lead–lag auxiliary controller is designed. The parameters of the lead–lag controller are determined by a pole assignment method based on the modal control theory [11].

2 Equivalent circuit of BES

The equivalent configuration of a BES is shown in Fig. 1, that containing a Y–Δ transformer, a converter, a battery

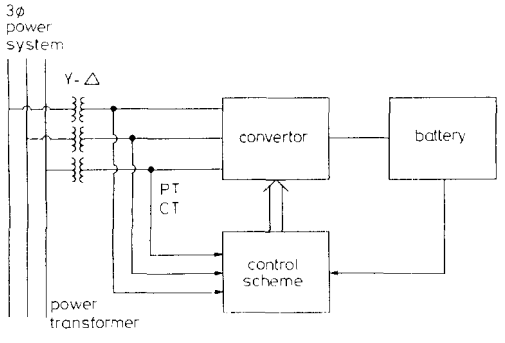

Fig. 1 *Configuration of BES*

and a control scheme. The converter is an interface between the three phase AC power system and the DC battery. The equivalent battery is composed of a set of batteries in parallel/series connection. The equivalent circuit of the BES can be represented by a converter connecting an equivalent battery as shown in Fig. 2, where

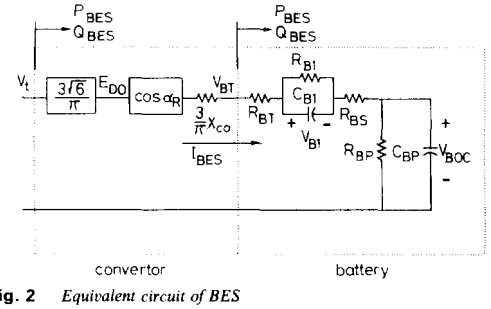

Fig. 2 *Equivalent circuit of BES*

E_{DO} is the ideal no-load maximum DC voltage of the converter. According to the converter circuit analysis

$$E_{DO} = \sqrt{(2)}V_{L-L}\frac{q}{\pi}\sin\frac{\pi}{q} = \sqrt{(6)}V_{L-N}\frac{q}{\pi}\sin\frac{\pi}{q} \tag{1}$$

where

q = pulse number

V_{L-L} = line to line RMS voltage

V_{L-N} = line to neutral RMS voltage

In this paper we simply consider a six-pulse converter, that is

$$E_{DO} = \frac{3\sqrt{(6)}}{\pi}V_{L-N} = \frac{3\sqrt{(6)}}{\pi}V_t \tag{2}$$

If X_{CO} is the commutating reactance of the converter, the equivalent commutating voltage drop of the six-pulse converter is $(3/\pi)X_{CO}I_{BES}$. The terminal voltage of the equivalent battery is obtained.

$$V_{BT} = \frac{3\sqrt{(6)}}{\pi}V_t\cos\alpha_R - \frac{3}{\pi}X_{CO}I_{BES} \tag{3}$$

Since the battery is an energy storage unit, its energy is represented in kWh. When a capacitor is used to model the battery unit, the capacitance can be determined from

$$\tfrac{1}{2}C_{BP}(V^2_{BOC,max} - V^2_{BOC,min}) = \text{kWh} \times 3600 \times 10^3 \tag{4}$$

Although C_{BP} is a function of voltage [8, 9], it is approximately a constant value during dynamic period, since the terminal voltage of the equivalent battery cannot change much for an instant. R_{BT} is the equivalent resistance of parallel/series connection batteries, and its value is dependent on the connecting conditions and amount of batteries. The parallel circuit of R_{B1} and C_{B1} is used to describe the energy and voltage during charging or discharging. R_{BP} is connected in parallel with C_{BP} to simulate the self-discharging of a battery. Since the self-discharging current of a battery is small, the resistance of R_{BP} is large.

We can obtain V_{BOC} and V_{B1} from the analysis of the equivalent circuit.

$$C_{BP}\frac{dV_{BOC}}{dt} = I_{BES} - \frac{V_{BOC}}{R_{BP}} \tag{5}$$

$$C_{B1}\frac{dV_{B1}}{dt} = I_{BES} - \frac{V_{B1}}{R_{B1}} \tag{6}$$

where

$$I_{BES} = \frac{V_{BT} - V_{BOC} - V_{B1}}{R_{BT} + R_{BS}} \tag{7}$$

The active power and reactive power absorbed by or released from the BES are

$$P_{BES} = \frac{3\sqrt{(6)}}{\pi}V_t I_{BES}\cos\alpha_R \tag{8}$$

$$Q_{BES} = \frac{3\sqrt{(6)}}{\pi}V_t I_{BES}\sin\alpha_R \tag{9}$$

Because of the power consumption of the converter, the power factor of the battery can be represented as

$$\cos\phi_R = \frac{V_{BT}}{E_{DO}} = \frac{\pi V_{BT}}{3\sqrt{(6)}V_t} = \cos\alpha_R - \frac{X_{CO}I_{BES}}{\sqrt{(6)}V_t} \tag{10}$$

then

$$\phi_R = \cos^{-1}\left(\frac{V_{BT}}{E_{DO}}\right) = \cos^{-1}\left(\cos\alpha_R - \frac{X_{CO}I_{BES}}{\sqrt{(6)}V_t}\right) \tag{11}$$

Within the BES, the active power and reactive power absorbed by and released from the battery are

$$P_{DC} = V_{BT} I_{BES} = E_{DO} I_{BES} \cos \phi_R$$
$$= \frac{3\sqrt{(6)}}{\pi} V_t I_{BES} \cos \alpha_R - \frac{3}{\pi} X_{CO} I_{BES}^2$$
$$= P_{BES} - \frac{3}{\pi} X_{CO} I_{BES}^2 \quad (12)$$

$$Q_{DC} = E_{DO} I_{BES} \sin \phi_R$$
$$= \frac{3\sqrt{(6)}}{\pi} V_t I_{BES} \sin \left[\cos^{-1} \left(\cos \alpha_R - \frac{X_{CO} I_{BES}}{\sqrt{(6)} V_t} \right) \right] \quad (13)$$

3 Dynamic model of BES

To enable the BES model to be easily utilised in the stability analysis of a power system, the model should be given in the frequency domain as shown in Fig. 3. The control scheme lets the BES have the ability of active power and reactive power modulation according to system requirement. Since active power control affects the power system frequency directly, that is the speed of a generator here, the active power increment ΔP_{BES} transferred through the converter is controlled depending upon the measured frequency deviation or speed deviation of the turbogenerator rotor; that is

$$\Delta P_{BES} = \frac{K_{BP}}{1 + ST_{BP}} \Delta\omega \quad (14)$$

where K_{BP} and T_{BP} are the control loop gain and speed measurement device time constant, respectively. Since voltage regulation is obtained by reactive power control, the reactive power increment ΔQ_{BES} transferred through the converter is controlled depending on the terminal voltage deviation; that is

$$\Delta Q_{BES} = \frac{K_{BQ}}{1 + ST_{BQ}} \Delta V_t \quad (15)$$

where K_{BQ} and T_{BQ} are the control loop gain and voltage measurement device time constant, respectively.

The incremental values ΔP_{BES} and ΔQ_{BES} are added to the existing command of active power and reactive power, $P_{BES0}$and Q_{BES0}, to obtain the expected values of active power P^*_{BES} and reactive power Q^*_{BES}, respectively. The expected converter firing angle is

$$\alpha^*_R = \tan^{-1} \left(\frac{Q^*_{BES}}{P^*_{BES}} \right) \quad (16)$$

The actual firing angle can be obtained from

$$\alpha_R = \frac{K_R}{1 + ST_R} (\alpha^*_R - U_{BES} + K_M \Delta I_{BES}) \quad (17)$$

where T_R and K_R are the firing circuit delay tine constant and converter loop gain, respectively. U_{BES} is the output signal of an auxiliary controller for specified purposes. $K_M \Delta I_{BES}$ is used to stabilise the BES under contant current operation, where a BES can release more power from batteries. The sign of K_M is dependent on the firing angle position in the P–Q plane. K_M is positive in the first and third quadrants, and negative in the second and fourth quadrants.

The equivalent circuit of batteries in Fig. 2 also should be transformed into the frequency domain. Taking the Laplace transform of eqns. 5 and 6, we can obtain the values of V_{BOC} and V_{B1} in the frequency domain.

$$V_{BOC} = \frac{R_{BP}}{1 + SR_{BP} C_{BP}} I_{BES} \quad (18)$$

$$V_{B1} = \frac{R_{B1}}{1 + SR_{B1} C_{B1}} I_{BES} \quad (19)$$

With the other algebra equations for the converter and battery in Section 2, the dynamic model for a BES as shown in Fig. 3 can fully reveal the dynamic behaviour for a stability study. The input to the model includes five command signals, I_{BES0}, P_{BES0}, Q_{BES0}, ω_{ref}, and V_{ref}, two feedback signals, ω and V_t, and one auxiliary control signal, U_{BES}. The output from the model contains three BES values P_{BES}, Q_{BES} and I_{BES}, and two battery signals P_{DC} and Q_{DC}.

Fig. 3 is the block diagram of a BES dynamic model under charging mode. The discharging mode block diagram also can be derived with some modifications to

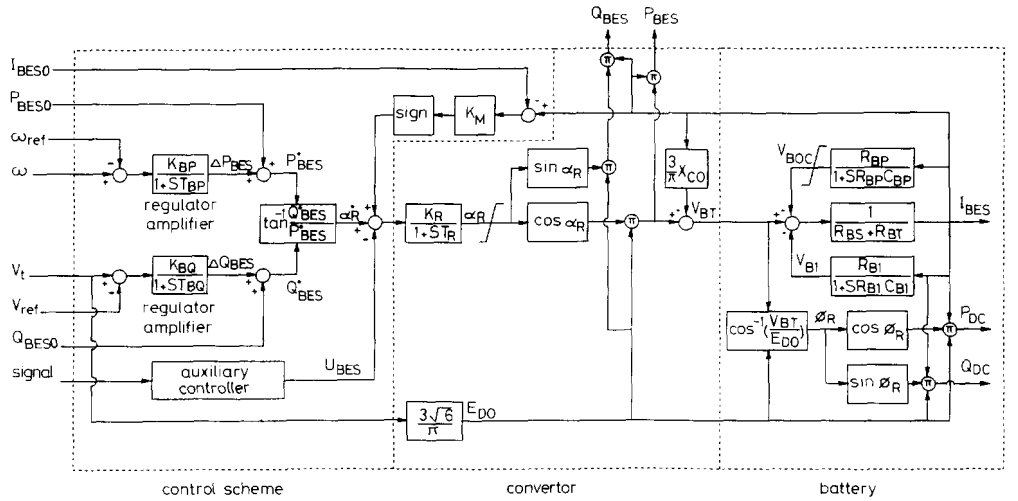

Fig. 3 *Block diagram of BES dynamic model*

Fig. 3. It is convenient to use the ignition angle β_I for the converter in discharging mode [7]. The terminal voltage of the equivalent battery is

$$V_{BT} = E_{DO} \cos \beta_I - I_{BES} R_E$$
$$= \frac{3\sqrt{(6)}}{\pi} V_t \cos \beta_I - \frac{3}{\pi} X_{CO} I_{BES} \quad (20)$$

where $\beta_I = \pi - \alpha_R$. We can tabulate the difference between charging mode and discharging mode dynamic models in Table 1. For a discharging mode model, the modifications to Fig. 3 are as follows

Table 1: Differences between charging mode and discharging mode

Item	Charging mode	Discharging mode
Firing angle	α_R	$\beta_1 = \pi - \alpha_R$
P_{BES}	$\frac{3\sqrt{(6)}}{\pi} V_t I_{BES} \cos \alpha_R$	$\frac{3\sqrt{(6)}}{\pi} V_t I_{BES} \cos \beta_I$
Q_{BES}	$\frac{3\sqrt{(6)}}{\pi} V_t I_{BES} \sin \alpha_R$	$-\frac{3\sqrt{(6)}}{\pi} V_t I_{BES} \sin \beta_I$
I_{BES}	positive value	negative value
V_{B1}	positive value	negative value

Add a block of $\pi - \alpha_R$ between $K_R/(1 + ST_R)$ and the limiter; then the variable α_R in sin and cos arguments is replaced by β_I.

Change the sign of sin function; that is, $\sin \alpha_R$ is replaced by $-\sin \beta_I$ and $\sin \phi_R$ is replaced by $-\sin \phi_I$.

4 Connection to power system

In the stability study of a power system, the quantities of synchronous machines, transmission lines, loads and other devices are usually expressed in the two-axis frame [12]. The quantities in the *abc* frame can be transferred into the two-axis frame by Park's transformation.

$$V_{odq} = PV_{abc} \quad (21)$$

where P is the Park transformation matrix.

In the BES dynamic model, the output variables are P_{BES} and Q_{BES}. These quantities described by the BES terminal voltage and current in the two-axis frame are

$$P_{BES} = V_{td} I_{BESd} + V_{tq} I_{BESq} \quad (22)$$

$$Q_{BES} = V_{td} I_{BESq} - V_{tq} I_{BESd} \quad (23)$$

Where V_{td} and V_{tq} are the d-axis and q-axis components of V_t, respectively, and I_{BESd}, I_{BESq} are the d-axis and q-axis components of I_{BES}, respectively. Then the two-axis currents flowing into the BES are

$$I_{BESd} = \frac{V_{td} P_{BES} - V_{tq} Q_{BES}}{V_t^2} \quad (24)$$

$$I_{BESq} = \frac{V_{tq} P_{BES} + V_{td} Q_{BES}}{V_t^2} \quad (25)$$

where

$$V_t = (V_{td}^2 + V_{tq}^2)^{1/2} \quad (26)$$

In the stability applications, a BES can be thought of a current sink in charging mode, or a current source in discharging mode.

5 Application

This section describes the application of a BES in the damping improvement of synchronous generator torsional oscillations. The BES is used as a damping device to give an additional damping torque to the power system. Both the BES and the power system are described in first-order nonlinear differential equations. In the eigenvalue analysis, those equations are linearised under an operating conditions to obtain a set of first-order linear differential equations. A scientific computer package is used to calculate the system eigenvalues. In the time-domain dynamic simulations, nonlinear differential equations are solved by a fourth-order Runge–Kutta method.

5.1 Studied system

The system under study is the IEEE Second Benchmark Model, system 1 [10] as shown in Fig. 4, where a generator supplies power to the infinite bus through two long-distance AC lines. One line is with series capacitor compensation. A BES is located at the generator bus terminal to provide active power and reactive power modulation. The dynamic behaviour of the generator is described by the nonlinear full current model. The IEEE type 1 excitation system [12] supplies the field current to the generator. All system data are given in the Appendix.

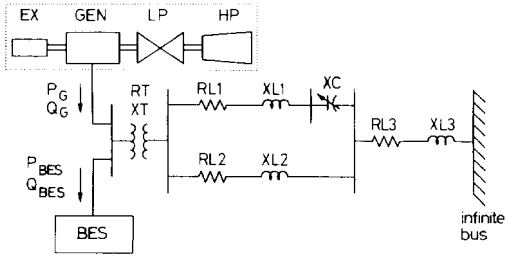

Fig. 4 *The IEEE second benchmark model system 1 with a BES*

5.2 Eigenvalues analysis

The complete eigenvalues of the open-loop system, that is without the BES, are listed in the first column of Table 2. The torsional oscillations are dominated by mode 0 to mode 3 (torsional modes). It is observed that mode 1 is unstable and modes 2 and 3 are nearly undamped. When the BES under charging mode is incorporated into the power system, all eigenvalues are listed in the second column of Table 2. It is shown that the system with the BES alone has a little damping improvement, but still has insufficient damping for torsional modes. As a result, some additional control signal can be added into the BES control scheme to damp out the torsional oscillations resulted from the negative damping modes. In this paper a lead–lag controller with the following transfer function and the generator speed feedback is proposed to increase the damping of mode 1 and mode 2.

$$\frac{U_{BES}}{\Delta\omega} = \frac{SK_W}{1 + ST_W} \frac{1 + ST_2}{1 + ST_1} \quad (27)$$

The parameters of the lead–lag controller are determined by the pole-assignment method based on the modal control theory [11]. We can obtain the parameters of the controller from a simple matric operation by shifting the unstable eigenvalues of mode 1 and mode 2 to the prespecified position. The result is listed as follows. Prespeci-

Table 2: The system eigenvalues

Modes	Without BES	Charging mode		Discharging mode	
		with BES but without lead–lag controller	with BES and lead–lag controller	with BES but without lead–lag controller	with BES and lead–lag controller
Mode 0	$-0.2139 \pm j8.87$	$-0.4986 \pm j9.655$	$-0.8513 \pm j9.007$	$-0.4384 \pm j9.64$	$-0.7459 \pm j8.921$
Mode 1	$0.5014 \pm j155.44$	$0.3878 \pm j155.47$	$-3.414 \pm j155.15$	$0.4725 \pm j155.37$	$-7.112 \pm j150.36$
Mode 2	$-0.046 \pm j203.46$	$-0.0467 \pm j203.47$	$-1.0 \pm j203.1$	$-0.0459 \pm j203.45$	$-1.5774 \pm j203.29$
Mode 3	$-0.0522 \pm j321.13$	$-0.054 \pm j321.13$	$-0.3993 \pm j321.11$	$-0.0538 \pm j321.13$	$-0.5817 \pm j321.42$
Other modes	$-15.61 \pm j605.43$	$-17.36 \pm j605.53$	$-17.55 \pm j605.59$	$-15.65 \pm j605.51$	$-15.90 \pm j605.69$
	$-21.56 \pm j376.56$	$-10.14 \pm j376.54$	$-0.8137 \pm j376.03$	$-20.07 \pm j376.21$	$-7.604 \pm j367.87$
	$-15.62 \pm j148.32$	$-17.53 \pm j147.7$	$-18.61 \pm j149.47$	$-16.35 \pm j147.84$	$-15.9 \pm j152.36$
	$-28.71 \pm j11.67$	$-28.99 \pm j11.49$	$-29.0 \pm j11.48$	$-26.73 \pm j10.54$	$-26.65 \pm j10.64$
	$-19.21 \pm j0.9517$	$-19.36 \pm j5.264$	$-19.49 \pm j5.313$	$-23.37 \pm j5.16$	$-23.6 \pm j4.932$
	$-1.536 \pm j0.402$	$-1.275 \pm j0.606$	$-1.274 \pm j0.605$	$-1.033 \pm j0.659$	$-1.033 \pm j0.656$
	-5.367	-5.208	-5.212	-4.822	-4.837
		-1029	-1029	-1023	-1019
		-996.5	-995.1	-996.0	-993.2
		-38.69	-38.69	-48.0	-48.05
		-38.46	-38.46	-38.46	-38.46
		-0.000331	-0.000331	-0.000325	-0.000325
			-117.8		-123.2
			-9.057		-9.088

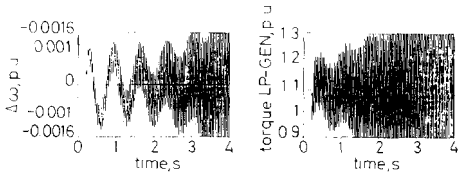

Fig. 5 *Dynamic responses of the system without BES*

fied eigenvalues

$-3.414 \pm j155.15$ (mode 1)

$-1.0 \pm j203.1$ (mode 2)

Parameters of lead–lag controller

$T_1 = 0.00893$ s

$T_2 = 0.0203$ s

$T_W = 0.1215$ s

$K_W = 40.65$ s

The eigenvalues of the system with the BES and the lead–lag controller are given in the third column of Table 2. It can be observed that mode 1 and mode 2 are exactly at the assigned position. Although we primarily want to enhance the damping of these two modes, the other torsional modes also benefit the damping effect. It is valuable to note that the damping of the electromechanical mode (mode 0) is simultaneously greatly improved.

It is worth examining the effect of the BES under discharging mode on damping the torsional oscillations. When the discharging mode BES is incorporated into the power system, all eigenvalues are also listed in the fourth column of Table 2. The system only has a little damping improvement as the same by the charging mode. Incorporating the above lead–lag controller designed under charging mode, all eigenvalues are listed in the fifth column of Table 2. The damping of all torsional modes is greatly improved.

It has been examined, but is not revealed here, that the BES with the lead–lag controller can ensure good damping for the power system under various operating points.

5.3 Dynamic simulations

Since the eigenvalues analysis are performed based on the linearised model, dynamic simulations using nonlinear differential equations are taken to ensure the damping

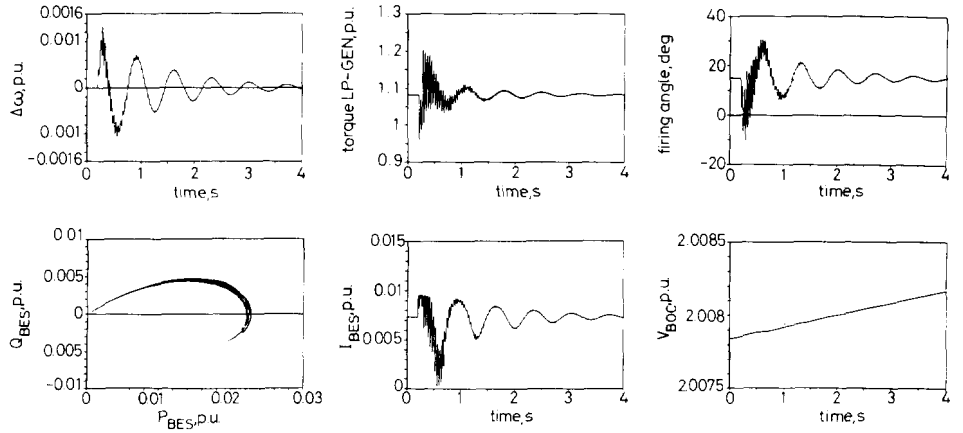

Fig. 6 *Dynamic responses of the system with BES and auxiliary controller in charging mode*

effect declared in the eigenvalues analysis. All nonlinearities, such as exciter ceiling voltage limits and battery open-circuit voltage limits, must be included. A 0.1 p.u. four-cycle mechanical torque change is used as a disturbance.

The dynamic responses of the system without the BES are shown in Fig. 5. The responses of the system with the BES and the lead–lag controller are shown in Figs. 6 and 7 in charging mode and discharging mode, respectively. In both operating modes the torsional oscillations can be effectively suppressed by the BES; that is, with the same result as in Table 2. During the dynamic period, the BES can draw active power and reactive power from the power system or release them, according to the system requirement.

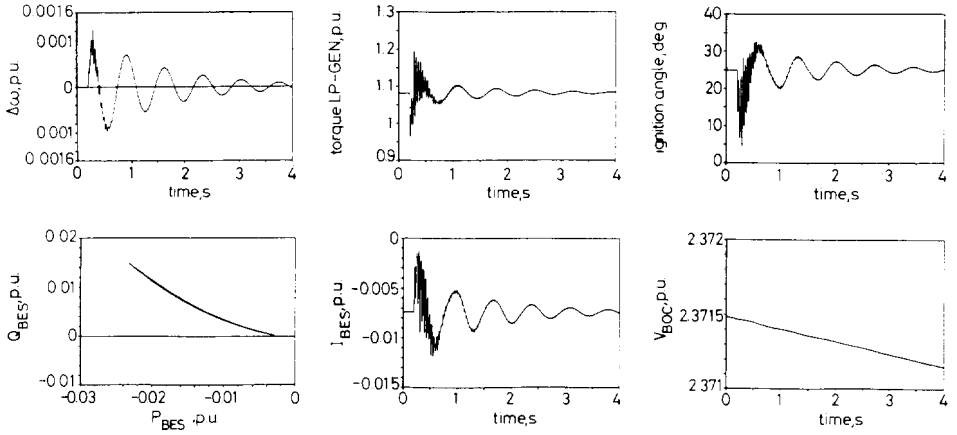

Fig. 7 *Dynamic responses of the system with BES and auxiliary controller in discharging mode*

6 Conclusions

In this paper a dynamic model of a BES is presented. The model is expressed in the frequency domain and can be easily applied in the stability application of a power system. The control scheme let the BES have the ability of active power and reactive power modulation according to system requirement. In the dynamic period, the BES can be thought of a current sink in the charging mode or a current source in the discharging mode. To examine the dynamic behaviour of this model, the investigation into the damping of torsional oscillations is performed. The BES with an auxiliary lead–lag controller is proposed to enhance the torsional modes damping of the turbogenerator. Eigenvalues analysis and dynamic simulations shows that the torsional oscillations can be effectively suppressed. The dynamic performance of the power system is greatly improved.

Until now there have been some commercial applications of the BES in Germany [3], South Africa [13] and the USA [1, 2]. However, since there is more and more desire for better load management and electric power quality, the BES will receive more attention in the future. The investigations of the BES fall into two categories: modified lead–acid battery and advanced battery researches [14]; and BES control and operation technology researches. The establishment of the BES dynamic model can provide a basis for the control method development and the observation of responses and behaviour of batteries. Furthermore, it can be used to investigate the application of a BES in a power system.

7 References

1 PUBLIC SERVICE ELECTRIC & GAS CO.: 'Demonstration test of a 500-kW peak-shaving lead–acid battery energy storage system'. Project report AP-4841, Electric Power Research Institute, California, 1986

2 WALKER, L.H.: '10 MW GTO converter for battery peaking service', *IEEE Trans. Ind. Appl.*, 1990, **26**, (1), pp. 63–72

3 KUNISCH, H.J., KRAMER, K.G., and DOMINIK, H.: 'Battery energy storage, another option for load-frequency-control and instantaneous reserve', *IEEE Trans. Energy Convers.*, 1986, **1**, pp. 41–46

4 BRAUNER, G., PESCH, H., and WAHI, A.: 'Leistungssteuerung und Verbesserung der dynamischen Stabilität in Industrienetzen durch Batteriespeicheranlagen', *Sonderdruck aus Elektrizitätswirtschaft*, 1989, Jg. 88, Heft 10

5 BECK, J.W., CARROL, D.P., GAREIS, G.E., KRAUSE, P.C., and ONG, C.M.: 'A computer study of battery energy storage and power conversion equipment operation', *IEEE Trans. Power Appar. Syst.*, 1976, **95**, pp. 1064–1072

6 GAREIS, G.E., CARROLL, D.P., ONG, C.M., and WOOD, P.: 'The interaction of battery and fuel cells with electrical distribution system: force commutated converter interface', *IEEE Trans. Power Appar. Syst.*, 1977, **96**, (4), pp. 1242–1250

7 KIMBARK, E.W.: 'Direct current transmission' (John Wiley, 1971), Vol. 1

8 SALAMEH, Z.M., CASACCA, M.A., and LYNCH, W.A.: 'A mathematical model for lead–acid batteries', *IEEE Trans. Energy Convers.*, 1992, **7**, pp. 93–98

9 CASACCA, M.A., LYNCH, W.A., and SALAMEH, Z.M.: 'Determination of lead–acid battery capacity via mathematical modelling techniques', *IEEE Trans. Energy Convers.*, 1992, **7**, pp. 442–446

10 IEEE SSR WORKING GROUP: 'Second benchmark model for computer simulation of subsynchronous resonance', *IEEE Trans. Power Appar. Syst.*, 1985, **104**, pp. 1057–1066

11 WU, C.J., and LEE, Y.S.: 'Application of simultaneous active and reactive power modulation SMES unit on the damping of turbogenerator subsynchronous oscillations', *IEEE Trans. Energy Convers.*, 1993, **8**, pp. 63–70

12 ANDERSON, P.M., and FOUAD, A.A.: 'Power system control and stability' (The Iowa State University Press, Ames, 1977)

13 LACHS, W.R., and SUTANTO, D.: 'Battery storage plant within large centre', *IEEE Trans. Power Syst.*, 1992, **7**, (2), pp. 762–769

14 ENERGY DEVELOPMENT ASSOCIATES: 'Development of the zinc chloride battery for utility applications'. Project report AP-5018, Electric Power Research Institute, California, 1987

8 Appendix

BES (40 MWh) [2, 5, 6]

Battery voltages = 1755–2925 V DC

$X_{CO} = 0.0274\ \Omega$	$C_{BP} = 52\,600$ F
$C_{B1} = 1$ F	$R_{BT} = 0.0167\ \Omega$
$R_{BP} = 10\ \text{k}\Omega$	$R_{B1} = 0.001\ \Omega$
$R_{BS} = 0.013\ \Omega$	$K_{BP} = K_{BQ} = 1.06$
$T_{BP} = T_{BQ} = 0.026$ s	$K_M = 0.5$
$K_R = 1.0$	$T_R = 0.001$ s

Power system

Synchronous generator (p.u.) (600 MVA, 22 kV/500 kV) [10]

$X_{fd} = 1.6286$	$X_{fq} = 1.861$	$X_{kd} = 1.642$
$X_{kq} = 1.5238$	$X_{ad} = 1.51$	$X_{aq} = 1.45$
$X_d = 1.65$	$X_q = 1.59$	$R_a = 0.0045$
$R_{fd} = 0.00096$	$R_{fq} = 0.00898$	$R_{kd} = 0.016$
$R_{kq} = 0.0116$	$R_T = 0.0012$	$X_T = 0.12$
$R_{L1} = 0.0444$	$R_{L2} = 0.0402$	$X_{L3} = 0.18$
$X_{L1} = 0.48$	$X_{L2} = 0.4434$	$R_{L3} = 0.0084$

Mass-spring system (600 MVA, 22 kV) [10]

$M_H = 0.4982$ s $D_H = 0.0498$ p.u.

$K_{HL} = 42.69$ p.u./rad

$M_L = 3.102$ s $D_G = 0.3103$ p.u.

$K_{LG} = 83.46$ p.u./rad

$M_G = 1.759$ s $D_X = 0.176$ p.u.

$K_{GX} = 3.74$ p.u./rad

$M_x = 0.0138$ s $D_X = 0.00138$ p.u.

Exciter and voltage regular [12]

$K_A = 400$ $K_{EX} = 1.0$ $K_F = 0.03$ s

$T_A = 0.02$ s $T_{EX} = 0.8$ s $T_F = 1.0$ s

$A_{EX} = 0.098$ $B_{EX} = 0.553$

The initial operating conditions

$P_G = 0.9$ p.u. $PF = 0.9$ lagging $V_t = 1.0$ p.u.

$X_C/X_{L1} = 0.55$ $I_{BES} = 4.426$ kA $\alpha_R = 15°$

$\beta_I = 25°$